# Optical properties of MOVPE-grown ZnS epilayers on (100) GaAs

M. Fernández, P. Prete, N. Lovergine, A. M. Mancini, and R. Cingolani
*Istituto Nazionale di Fisica della Materia, Dipartimento di Scienza dei Materiali, Università di Lecce, Via Arnesano, I-73100 Lecce, Italy*

L. Vasanelli*
*IME-CNR, Via Arnesano, I-73100 Lecce, Italy*

M. R. Perrone
*Dipartimento di Fisica, Università di Lecce, Via Arnesano, I-73100 Lecce, Italy*

(Received 22 July 1996)

Excitonic properties of high-quality ZnS layers grown by low-pressure metal-organic vapor-phase epitaxy have been investigated using photoluminescence and absorption spectroscopy. Comparison with theoretical models has provided accurate information on eigenstates, broadening, strain, and temperature dependence of heavy-hole, light-hole, and split-off-band exciton transitions. Finally, radiative recombination due to inelastic exciton-polariton scattering is shown under strong injection rates. [S0163-1829(97)04807-8]

## I. INTRODUCTION

The achievement of efficient ultraviolet (UV) and blue-light-emitting diodes and lasers is one of the major challenges of modern optoelectronics. Among II–VI materials, ZnS is a potential candidate for applications to devices emitting in the UV and deep-blue-light spectral region, its room-temperature band-gap energy being 3.74 eV.

In addition, excitons in ZnS/GaAs heterostructures are expected to play an important role in optical transitions by virtue of the large binding energy (38 meV) comparable to the LO-phonon energy (43.6 meV).

We have previously reported on the metal-organic vapor-phase epitaxy (MOVPE) growth of ZnS epilayers, describing how they were optimized by a suitable choice of precursors and growth conditions.[1,2] The aim of this paper is to analyze the linear optical properties of our samples in order to provide a detailed description of the excitonic states by means of absorption and photoluminescence (PL) spectroscopy. Although excitonic features have been previously reported,[3,4] this systematic study has been carried out on high-quality epitaxial structures, providing a determination of the fundamental excitonic parameters, namely, eigenstates, strain effects, thermal broadening, and split-off bands. Moreover, we investigated nonlinear phenomena that appear under strong photogeneration rate, and determined the threshold excitation intensity beyond which inelastic exciton-polariton scattering becomes predominant over radiative decay of excitons.

## II. EXPERIMENTAL DETAILS

High-quality ZnS epilayers have been grown on (100) GaAs by means of an Aixtron 200RD MOVPE reactor, by using tertiary-buthyl-mercaptan [(*t*-Bu)SH] and dimethylzinc:triethylammine ($Me_2Zn:Et_3N$) adduct as S and Zn precursors, respectively.[1] Semi-insulating liquid-encapsulated Czchocralski (LEC)-grown (100)$\pm 0.25°$ oriented GaAs wafers were used as substrates. Before being loaded into the reactor chamber, the substrates were chemically etched for 8 min by dipping in a $H_2SO_4:H_2O_2:H_2O$ (4:1:2) solution kept at 40 °C. An *in situ* thermal treatment under $H_2$ flow was then performed on the GaAs at 550 °C for about 30 min immediately before the growth,[2] in order to remove the oxide left on the GaAs surface by the etching process, as well as to restore the GaAs surface stoichiometry. The MOVPE growth of ZnS was performed under a 304-mbar total chamber pressure and 342 °C temperature. The transport rates of $Me_2Zn:Et_3N$ and (*t*-Bu)SH were chosen to achieve precursors molar flow ratios ($\mathrm{MFR}=F_{(t-\mathrm{Bu})\mathrm{SH}}/F_{\mathrm{Me_2Zn:Et_3N}}$) around 5.0.

Absorption measurements were performed in the temperature range 10–300 K in the near-band-edge region of ZnS. To this purpose, a $\sim$100-$\mu$m-diameter pin hole was obtained by partly removing the GaAs substrate from the back of each sample, following a procedure described elsewhere.[5] The light beam of a 1-kW Xe lamp was then focused onto the sample, the transmitted light being dispersed by a 0.85-m double monochromator, and finally detected by a cooled GaAs photon counting. The overall spectral resolution of the absorption measurements was always better than 0.5 meV.

High-resolution continuous wave PL measurements were carried out using the UV line (1 W at 275.4 nm) of a large frame $Ar^+$ laser, by using the same detection system described above in a backscattering configuration. Finally, high-excitation intensity PL spectra were recorded by using a XeCl-excimer laser (308 nm) with 20-ns pulse duration and pulse intensities of 300 $kW/cm^2$. The detected radiation was dispersed by a 0.25-m monochromator with a grating of 2400 lines/mm, providing a resolution better than 2 meV.

## III. RESULTS AND DISCUSSION

### A. Absorption spectroscopy

A typical 10-K absorption spectrum of a 0.87-$\mu$m-thick ZnS epilayer is displayed in Fig. 1 (squares) together with

0163-1829/97/55(12)/7660(7)/$10.00 55 7660 © 1997 The American Physical Society

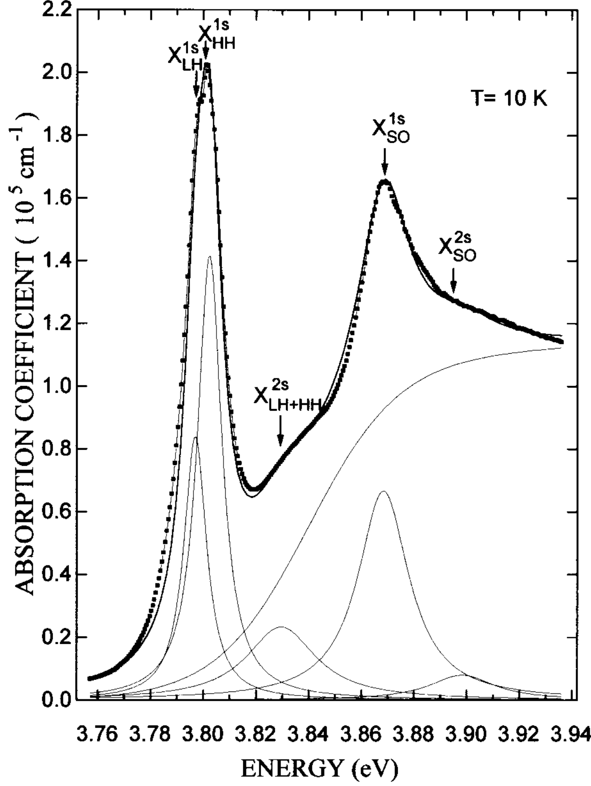


FIG. 1. Absorption spectrum at 10 K from a 0.87-$\mu$m-thick ZnS/GaAs heterostructure (solid squares). The best fit of the data is shown (thick solid line) together with the individual $1s$ and $2s$ heavy-hole (HH), light-hole (LH) and split-off (SO) absorption resonances and continuum edge including the Sommerfeld factor (thin solid lines).

the calculated line shape (continuous curve). Unprecedently sharp exciton resonances associated with the heavy-hole ($X_{\mathrm{HH}}^{1s}$) and light-hole ($X_{\mathrm{LH}}^{1s}$) doublets (splitted by the strain) along with the split-off-band resonance ($X_{\mathrm{SO}}^{1s}$) can be observed around 3.80 and 3.87 eV, respectively. The interband continuum, convoluted with the $2s$ state of the ground level HH and LH excitons ($X_{\mathrm{LH+HH}}^{2s}$) are clearly observed around 3.83 eV. Furthermore at 3.90 eV there is another structure, probably due to the excited states of the split-off band ($X_{\mathrm{SO}}^{2s}$).

The calculated absorption spectrum in Fig. 1 is obtained from the best fit of the experimental data to the following equation:

$$\alpha(E)=\sum_{n,i} L(E-E_i^{\mathrm{ns}},\alpha_i^{\mathrm{ns}},\Gamma_i^{\mathrm{ns}}) + \frac{\alpha_\infty}{1+\exp[-(E-E_g)/kT]}\,\frac{\exp(\pi\gamma^{1/2})}{\mathrm{senh}(\pi\gamma^{1/2})}, \quad (1)$$

where $i$ is a band index, $n$ is the principal quantum number ($1s$ or $2s$ exciton), $L(E-E_i^{\mathrm{ns}},\alpha_i^{\mathrm{ns}},\Gamma_i^{\mathrm{ns}})=\alpha_i^{\mathrm{ns}}/(1+[(E-E_i^{\mathrm{ns}})/\Gamma_i^{\mathrm{ns}}])$ is the Lorentzian function describing the exciton density of states, and $\gamma=(E_{\mathrm{hh}}^{1s}/|E-E_g|)$ is the residual electron-hole interaction (Sommerfeld factor).

Lorentzian functions[6] have been taken for the exciton density of states at low temperatures, whereas the absorption continuum has been fitted by a Fermi function corrected by the Sommerfeld factor,[7,8] which takes into account the residual Coulomb interaction between holes and electrons. In Table I we report the characteristic parameters obtained from the line-shape fitting of the experimental absorption curves. The binding energy of the $1s$ heavy-hole exciton is found to be $E_b^{1s}=(38\pm1)$ meV, while for the $2s$ exciton it corresponds to $E_b^{2s}=(10\pm2)$ meV, which is in good agreement with the Wannier's model and with PL excitation spectroscopy measurements.[9] A spin-orbit coupling[10] of about 66 meV is also evaluated through the split-off-band separation; this value is lower than those obtained by reflection spectroscopy.[4]

TABLE I. Characteristic parameters for LH, HH, and SO $1s$ and $2s$ excitons and for the absorption edge.

| | |
|---|---|
| $E_{\mathrm{lh}}^{1s}=(3.7970\pm0.0005)$ eV | $\Gamma_{\mathrm{lh}}^{1s}=(5.2\pm0.2)$ meV |
| $E_{\mathrm{hh}}^{1s}=(3.8024\pm0.0003)$ eV | $\Gamma_{\mathrm{hh}}^{1s}=(5.6\pm0.1)$ meV |
| $E_{\mathrm{so}}^{1s}=(3.8680\pm0.0004)$ eV | $\Gamma_{\mathrm{so}}^{1s}=(12\pm1)$ meV |
| $E_{\mathrm{lh+hh}}^{2s}=(3.830\pm0.001)$ eV | $\Gamma_{\mathrm{lh+hh}}^{2s}=(16\pm1)$ meV |
| $E_{\mathrm{so}}^{2s}=(3.898\pm0.001)$ eV | $\Gamma_{\mathrm{so}}^{2s}=(15\pm1)$ meV |
| $E_g=(3.840\pm0.001)$ eV | |

It is worth noting that the LH-HH energy splitting obtained from the fitting (5 meV) can be directly compared to the exciton splitting induced by the elastic strain, according to the Hamiltonian of Pikus and Bir.[11] This provides a quantitative estimate of the amount and sign of the crystal strain. The energy shifts calculated for LH, HH, and SO bands are given by[12]

$$\Delta E_{\mathrm{hh}}^{1s}=\left[2a-b-2(a+b)\,\frac{C_{12}}{C_{11}}\right]\varepsilon_\parallel=-0.58\varepsilon_\parallel, \quad (2a)$$

$$\Delta E_{\mathrm{lh}}^{1s}=\left[2a+b-2(a-b)\,\frac{C_{12}}{C_{11}}\right]\varepsilon_\parallel-\frac{2b^2}{\Delta_0}\left[\frac{C_{11}+2C_{12}}{C_{11}}\right]^2\varepsilon_\parallel^2 =-6.21\varepsilon_\parallel-226\varepsilon_\parallel^2, \quad (2b)$$

$$\Delta E_{\mathrm{so}}^{1s}=\left[2a\,\frac{C_{11}-C_{12}}{C_{11}}\right]\varepsilon_\parallel+\frac{2b^2}{\Delta_0}\left[\frac{C_{11}+2C_{12}}{C_{11}}\right]^2\varepsilon_\parallel^2 =-3.40\varepsilon_\parallel+226\varepsilon_\parallel^2, \quad (2c)$$

where $C_{ij}$ are the elastic stiffness constants of ZnS,[13] $a$ the hydrostatic deformation potential,[14] and $b$ the valence-band shear deformation potential.[15] The quadratic terms in Eqs. (2b) and (2c) are due to spin repulsion between LH and SO bands. With the data of Table I one obtains a value of tensile strain for the LH band that is equal to $(1.5\pm0.3)\times10^{-3}$ and for the split-off band $\varepsilon_\parallel=(1.3\pm0.6)\times10^{-3}$. These strain values are in good agreement with the expected value of the built-in thermal strain ($1.47\times10^{-3}$) arising by cooling down the samples from the growth temperature to 10 K and due to the different linear thermal expansion coefficients of ZnS and GaAs. Thus the original lattice mismatch of the heterostructure (4.6% at room temperature) has been completely relaxed at the thickness of our samples, which is very large with respect to the ZnS critical thickness (of the order of $h_c\sim1$–4 nm).[16,17] Results on ZnS layers grown on GaP have also been reported recently.[18] In this case the lattice

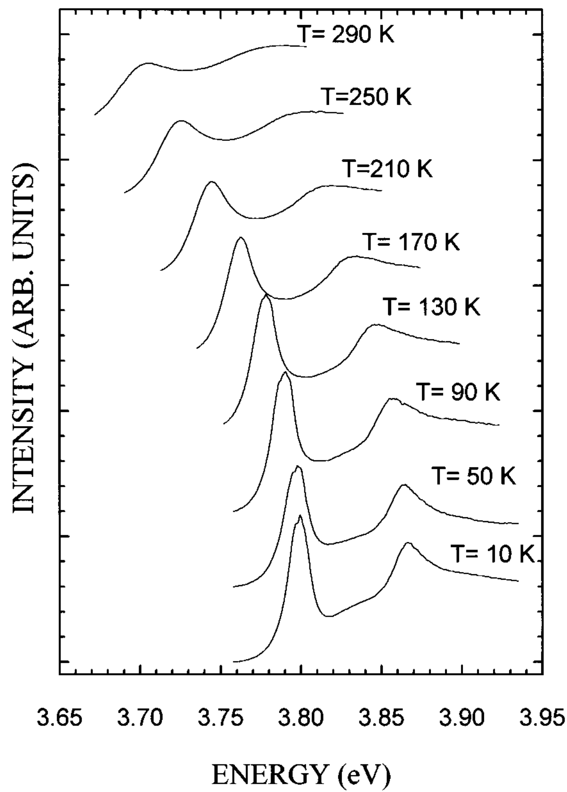


FIG. 2. Temperature-dependent absorption spectra of a ZnS/GaAs sample.

mismatch is much smaller than the ZnS/GaAs heterostructure, and the strain relaxation dynamics is not comparable to the results presented here.

Systematic absorption measurements have also been performed in the 10–300-K temperature range (Fig. 2). With increasing temperature the exciton resonances lose oscillator strength, due to thermal dissociation, and shift uniformly toward lower energies. The deconvolution between the LH and HH resonances becomes more and more difficult with increasing temperature, and the two peaks are not directly distinguishable for temperatures higher than 110 K, when thermal broadening effects become dominant. Nevertheless, a clear exciton feature can still be observed in our absorption spectra up to room temperature.

All temperature dependent spectra have been systematically analyzed using Eq. (1). Thermal effects, which modify the line shape of the exciton resonance, have been accounted for by means of Voigt functions, in which the relative weight of the Gaussian component increases with increasing temperature.

The results of this analysis are shown in Fig. 3 (symbols), where we plot the temperature dependence of the LH, HH and SO exciton eigenstates and linewidths [Figs. 3(a) and 3(b), respectively]. In the inset of Fig. 3(b) we report the temperature dependence of the Voigt parameter. As expected, the resonance transforms from predominantly Lorentzian at low temperature to predominantly Gaussian at high temperature.

The temperature dependence of the exciton energy typically shows two different asymptotic behaviors. At very low temperatures [well below the Debye temperature $T \ll \theta_D^{\mathrm{ZnS}} = 334$ K (Ref. 19)] the trend is $\propto T^4$ caused by electron-phonon scattering, while for temperatures higher than 80 K it becomes linear, due to lattice thermal expansion. This can be described by a modification of Varshni's semiempirical law[20] for semiconductors, which can be written as

$$E(T) = E(0) - \frac{\alpha T^4}{(\beta + T)^3}. \tag{3}$$

This function fits out data much better than any other expression used for ZnS,[3] as shown by the excellent comparison (continuous lines) with the experimental data displayed in Fig. 3(a).[21] Values of $\alpha$ and $\beta$ obtained by the fitting procedure, are reported in Table II, together with the slope $\xi$ of a linear fit using only data $>\beta$.

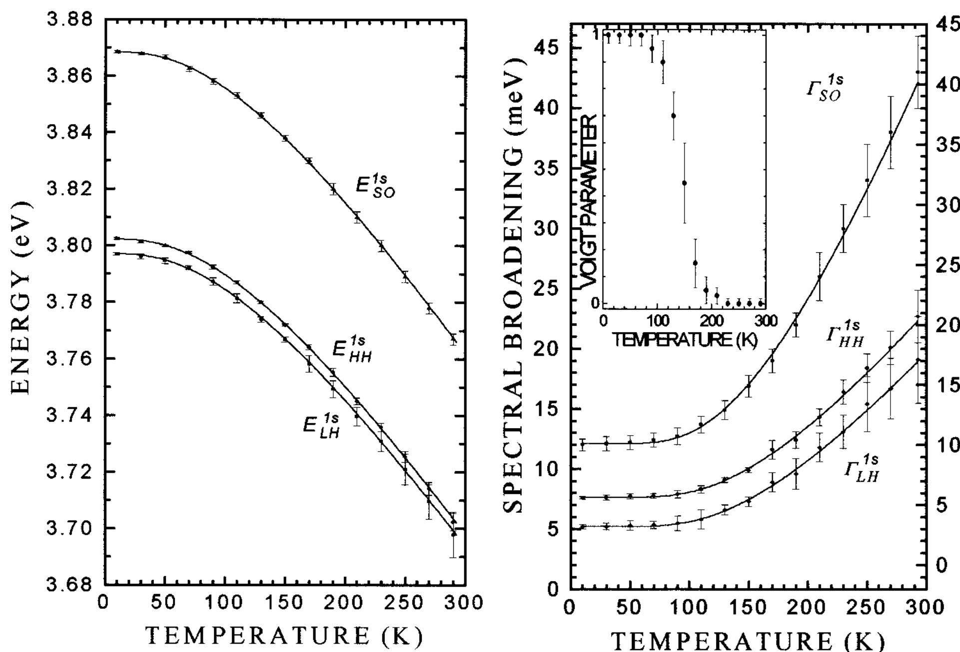


FIG. 3. LH, HH, and SO 1*s* exciton peak energy (a) and FWHM of the same peaks (b) as a function of temperature. Note that in (b) the HH curve has been offset by 2 meV (right-hand scale) compared with the LH and SO curves (left-hand scale) for a better visualization. Inset: Temperature dependence of the Voigt parameter obtained from the best fit of the absorption spectra. 0 means the Lorentzian function, whereas 1 indicates a fully Gaussian line shape.

TABLE II. Parameter values associated with Varshni's modified law, slope dependence for $T>\beta$, homogeneous ($\Gamma_{LO}$), and inhomogeneous ($\Gamma_{inh}$) broadening coefficients for LH, HH, and SO $1s$ excitons.

| | $E^{1s}(0)$ (eV) | $\alpha(\times 10^{-4}$ eV/K) | $\beta$ (K) | $\xi(\times 10^{-4}$ eV/K) | $\Gamma_{inh}$ (meV) | $\Gamma_{LO}$ (meV) |
|---|---|---|---|---|---|---|
| LH band | 3.7970±0.0003 | 6.7 ±0.1 | 75±2 | 4.4±0.1 | 5.2±0.1 | 64±5 |
| HH band | 3.8022±0.0002 | 6.86±0.09 | 76±2 | 4.5±0.1 | 5.6±0.1 | 68±3 |
| SO band | 3.8684±0.0003 | 7.0 ±0.2 | 77±3 | 4.6±0.1 | 12.1±0.2 | 139±7 |

The temperature dependence of the absorption linewidth, which is a measure of the actual strength of the exciton-phonon coupling, has been compared to the usual lifetime broadening model[22]

$$\Gamma(T)=\Gamma_{inh}+\frac{\Gamma_{LO}}{\exp(\hbar\omega_{LO}/k_BT)-1}, \tag{4}$$

where the inhomogeneous broadening $\Gamma_{inh}$ is temperature independent and it is substantially coincident with the low-temperature linewidth. The homogeneous term, proportional through $\Gamma_{LO}$ (Fröhlich coupling constant) to the LO-phonon population, becomes important at high temperatures. The calculated values of the LH, HH, and SO full width at half maximum (FWHM) (curves) are compared to the experiments (symbols) in Fig. 3(b). Taking for the LO-phonon energy $\hbar\omega_{LO}\sim 43.6$ meV (as measured by Raman scattering[23]), the excellent fit of Fig. 3(b) provides for $\Gamma_{inh}$ and $\Gamma_{LO}$ the values reported in Table II. The small value of the inhomogeneous broadening compared with those of other authors[3,4] demonstrates the high optical quality of the present ZnS epilayers. Conversely, the homogeneous term, has a relatively large value as compared to other II–VI heterostructures,[24,25] suggesting a stronger exciton-phonon coupling in ZnS.

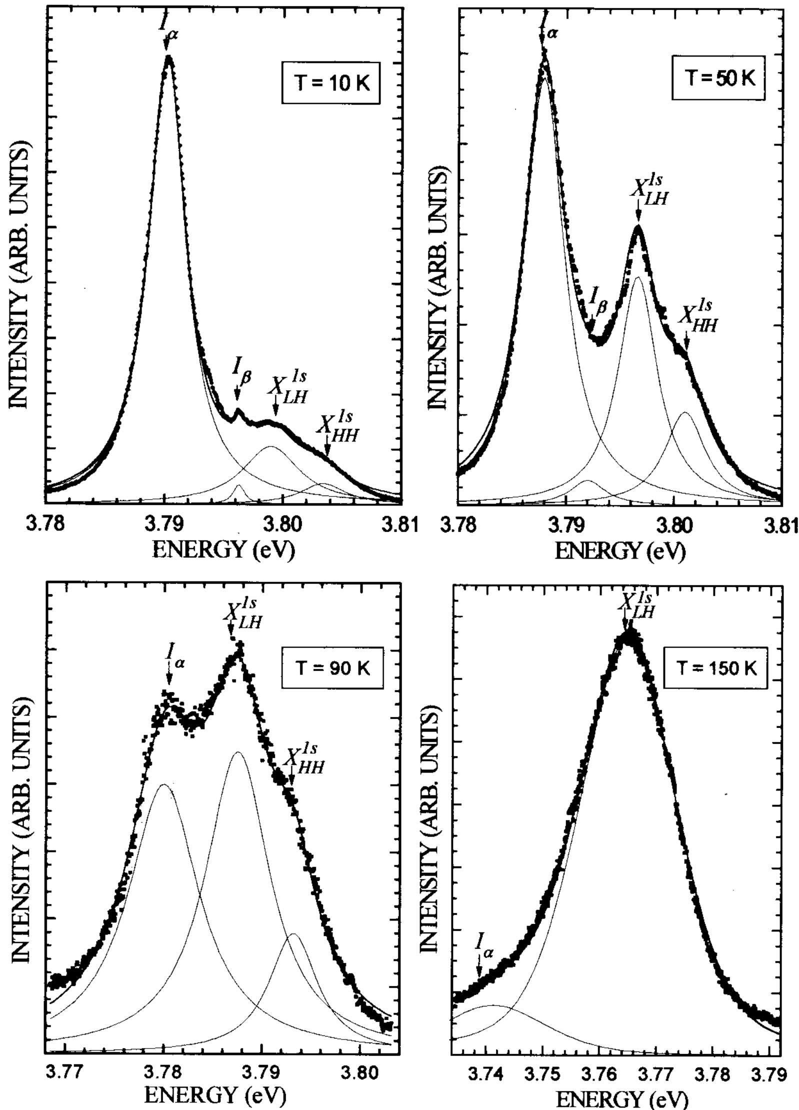


FIG. 4. Low-excitation intensity PL spectra for different temperatures. The impurity related peaks ($I_\alpha$ and $I_\beta$) smear out with increasing temperature, whereas the LH exciton resonance becomes predominant ($X^{1s}_{LH}$).

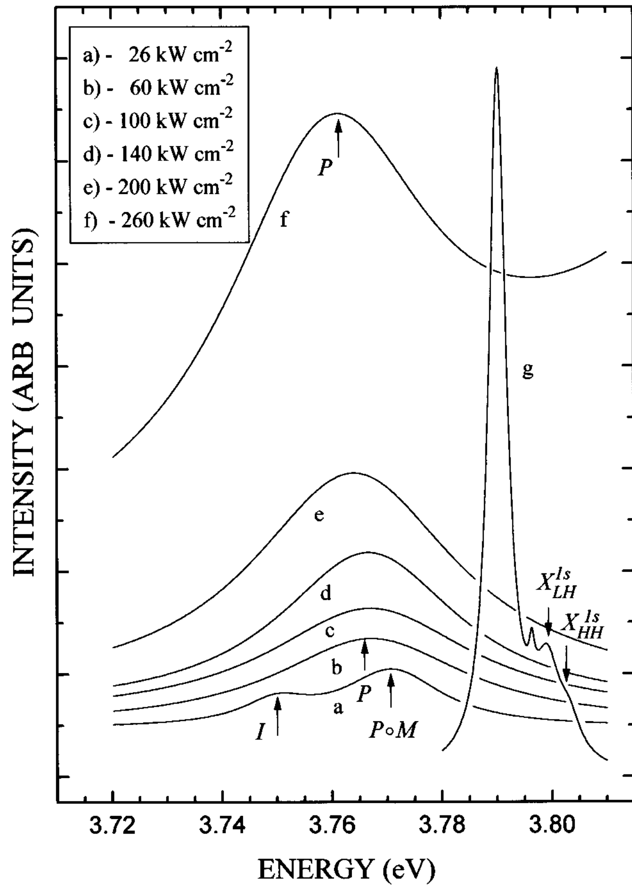


FIG. 5. High-excitation intensity PL spectra $(a-f)$ from a ZnS/GaAs sample at 10 K. The peak $P \cdot M$ is due to inelastic scattering between free excitons with excitation ($M$) and dissociation ($P$) [see Eqs. (5)], while $I$ corresponds to extrinsic emission. For comparison, a low excitation intensity PL spectrum ($g$, not to scale) is also reported.

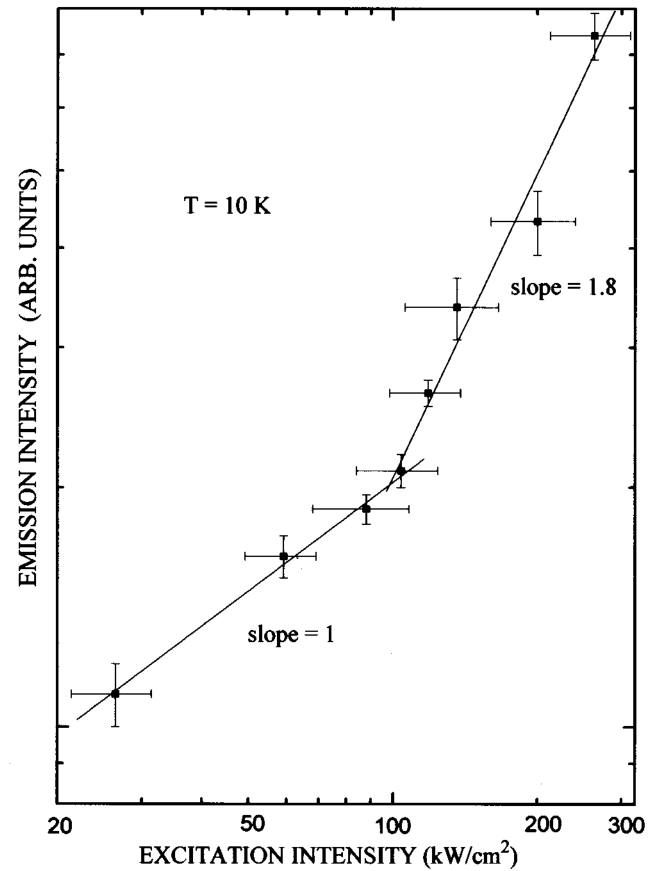


FIG. 6. Intensity of the $P$-band emission as a function of excitation intensity. Data have been fitted with two lines of linear and quadratic slope.

### B. Photoluminescence spectroscopy

Low-excitation high-resolution PL spectra have been measured in the near-band-edge region of ZnS between 10 and 300 K. Representative spectra are shown in Fig. 4 (symbols) together with a Voigt deconvolution of the principal features. At low temperatures (10 K) the dominant feature is a neutral donor bound exciton resonance ($I_\alpha$) at 3.790 eV which is attibuted to Cl impurities.[26] The presence of Cl in our samples has been independently confirmed by secondary-ion-mass spectrometry measurements.[27] The 3.799- and 3.803-eV peaks are assigned respectively to the LH and HH free excitons by comparison with absorption spectra. Finally, another bound exciton of lower intensity ($I_\beta$) appears at 3.796 eV.

With increasing temperature there is a progressive reduction of bound exciton resonances due to thermal ionization, and a concomitant enhancement of the $X_{\rm LH}^{1s}$, which dominates the spectrum for $T>90$ K. The LH and HH excitons can be resolved up to 130 K. Above this temperature a single-emission band can be measured up to room temperature.

In Fig. 5 we report some low-temperature PL emission spectra of ZnS under intense excitation (in the range 26–260 kW/cm$^2$). At the lowest intensity some extrinsic emission occurs ($I$) at 3.750 eV, this is found to saturate with increasing injection rate. A second peak ($P$) appears at 3.771 eV, which may be attributed to inelastic scattering between free excitons (FX). Further increase of excitation results in a redshift of the emission band up to 3.761 eV at 260 kW/cm$^2$. The Lorentzian fit of different experimental spectra provides the intensity dependence of the $P$ band displayed in Fig. 6. The trend is linear up to excitation intensities of 100 kW/cm$^2$, whereas for higher values it becomes quadratic.

The mean feature in the luminescence spectra (the peak labeled $P$) is caused by inelastic scattering of Wannier excitons.[28] This process may happen in two different ways; namely, by excitation (a) or by dissociation (b) of one exciton with simultaneous creation of a free-electron-hole pair. Schematically this can be represented by the following reactions:

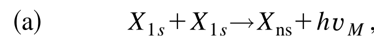

(a) $$X_{1s}+X_{1s}\rightarrow X_{\rm ns}+h\nu_M\,,$$

(b) $$X_{1s}+X_{1s}\rightarrow e^-+h^++h\nu_P\,.$$

Photons emerging from the sample in the two cases will be redshifted from the free exciton energy (3.803 eV) by an amount equal to

$$\Delta E_M=(1-1/n^2)E_B^X, \tag{5a}$$

$$\Delta E_P=E_B^X+E_k, \tag{5b}$$

where $E_B^X = 38$ meV represents the free exciton binding energy. In the first case [Eq. (5a)] the hole and electron remain in a bound state, so that the kinetic energy can be assumed to be negligible. Conversely, in Eq. (5b) the free electron-hole pairs have no restriction in their motion, and the kinetic term $E_k$ has to be accounted for.

According to this description, at the lowest excitation intensities (26 kW/cm$^2$) both processes of excitation and dissociation of excitons due to inelastic scattering are present in the PL spectra. The peak $P \cdot M$ in Fig. 5 (3.771 eV) is indeed caused by the convolution of the two processes. With increasing intensity the dissociation becomes predominant, while the process of excitation saturates. The redshift at very high intensities is due to the kinetic term, which becomes increasingly more important.

A further confirmation of the inelastic exciton scattering comes from the intensity dependence of the process displayed in Fig. 6. Actually, the rate equation which describes the emission intensities under stationary conditions is given by[29]

$$I = \frac{n_x}{\tau} + c n_x^2, \tag{6}$$

where $n_x$ is the concentration of excitons, which is proportional to the excitation intensity ($I_{\mathrm{exc}}$), $I$ is their rate of generation, $n_x/\tau$ is the radiative recombination rate, $\tau$ the mean lifetime of the excitonic level, and $c n_x^2$ the exciton-exciton interaction term. From Fig. 6 we observe that a linear dependence is observed up to 100 kW/cm$^2$, indicating predominant exciton recombination; for higher excitation intensities the quadratic dependence prevails, showing the role of inelastic scattering in the radiative recombination. The superlinearity of the PL intensity under high excitation suggests that stimulated emission and optical gain of excitonic origin may take place in ZnS.[30]

We should mention that previous papers have reported biexciton formation[30,31] and, in bulk ZnS, $e$-$h$ droplet (EHD) formation.[32,33] The former results cannot be invoked in our case due to the large shift of the $P$ band with respect to the band-gap edge.

The EHD formation is a more appealing candidate. In our experiment the $P$ band is observed up to relatively high temperatures, and, taking into account the short PL lifetime (not shown), we can hardly invoke an EH condensate. Nevertheless, EHD formation is likely to occur at liquid-He temperature in high-quality samples under intense photoexcitation.[32–34]

## IV. CONCLUSIONS

We reported a detailed study of the optical properties of high-quality ZnS/GaAs heterostructures grown by low-pressure MOVPE. We determined accurately the intrinsic properties of the ZnS epilayer, namely, LH, HH, and SO 1$s$ and 2$s$ exciton energy positions, broadening, temperature dependence, and residual built-in parallel strain in the structure. Moreover, by high-excitation PL we have observed interesting features on the spectra of our samples due to nonlinear effects like inelastic scattering of excitons.

## ACKNOWLEDGMENTS

We would like to acknowledge D. Cannoletta, A. Melcarne, M. Corrado, and A. Pinna for their technical help. Thanks are due to Dr. G. Leo, Dr. M. Mazzer, Dr. G. Imbriani, and Professor A. Drigo for several enlighting discussions. Epichem, Ltd. is also acknowledged for supplying the ($t$-Bu)SH source batch used in this work.

*Also with Istituto Nazionale di Fisica della Materia, Dipartimento di Scienza dei Materiali, Università di Lecce, Via Arnesano, I-73100 Lecce, Italy.

[1] N. Lovergine, M. Longo, C. Gerardi, D. Manno, A. M. Mancini, and L. Vasanelli, J. Cryst. Growth **156**, 45 (1996).

[2] G. Leo, N. Lovergine, P. Prete, M. Longo, R. Cingolani, A. M. Mancini, F. Romanato, and A. V. Drigo, J. Cryst. Growth **159**, 144 (1996).

[3] A. Abounadi, M. Di Blasio, D. Bouchara, J. Calas, M. Averous, O. Briot, N. Briot, T. Cloitre, R. L. Aulombard, and B. Gil, Phys. Rev. B **50**, 11 677 (1994).

[4] O. Briot, N. Briot, A. Abounadi, B. Gil, T. Cloitre, and R. Aulombard, Semicond. Sci. Technol. **9**, 207 (1994).

[5] R. Cingolani, P. Prete, D. Greco, P. V. Giugno, M. Lomascolo, R. Rinaldi, L. Calcagnile, L. Vanzetti, L. Sorba, and A. Franciosi, Phys. Rev. B **51**, 5176 (1995).

[6] Y. Toyozawa, Prog. Theor. Phys. **20**, 53 (1958).

[7] M. Shinada and M. Sunago, J. Phys. Soc. Jpn. **21**, 1936 (1966).

[8] R. J. Elliott, Phys. Rev. **108**, 1384 (1957).

[9] H. Kinto, M. Yagi, K. Tanigashira, T. Yamada, H. Uchiki, and S. Iida, J. Cryst. Growth **117**, 348 (1992).

[10] R. J. Elliott, Phys. Rev. **96**, 266 (1954).

[11] G. E. Pikus and G. L. Bir, Fiz. Tverd. Tela (Leningrad) **1**, 154 (1959); **1**, 1642 (1959) [Sov. Phys. Solid State **1**, 1502 (1959)]; G. E. Pikus, *ibid*. **6**, 324 (1963); G. E. Pikus and G. L. Bir, *Symmetry and Deformation Effects in Semiconductors* (Wiley, New York, 1974).

[12] F. H. Pollak and M. Cardona, Phys. Rev. **172**, 816 (1968).

[13] R. K. Singh and S. Singh, Phys. Status Solidi B **140**, 407 (1987).

[14] S. Ves, U. Schwartz, N. E. Christensen, K. Syassen, and M. Cardona, Phys. Rev. B **42**, 9113 (1990).

[15] K. Shahzad and D. Olego, Phys. Rev. B **38**, 1417 (1988).

[16] M. Henken, Mater. Sci. Eng. B **9**, 189 (1991).

[17] Z. P. Guan, S. H. Song, G. H. Fan, X. W. Fan, Y. G. Peng, and Y. K. Wu, J. Cryst. Growth **138**, 534 (1994).

[18] K. B. Ozanyan, L. May, J. E. Nicholls, J. H. C. Hogg, W. E. Hagston, B. Lunn, and D. E. Ashenford, J. Cryst. Growth **159**, 89 (1996).

[19] Y. K. Vekilov, A. P. Rusakov, Fiz. Tverd. Tela (Leningrad) **13**, 1157 (1971) [Sov. Phys. Solid State **13**, 956 (1972)].

[20] Y. P. Varshni, Physica **34**, 149 (1967).

[21] The linear and quadratic terms in the denominator of Eq. (3) allow the $\chi^2$ value of the fitting to be reduced by one order of magnitude compared to other expressions (cf. Ref. 3).

[22] A. Shen, L. Xu, H. Wang, Y. Chen, Z. Wang, and A. Z. Li, J. Cryst. Growth **127**, 383 (1993).
[23] G. W. Nilsen, Phys. Rev. **182**, 838 (1969).
[24] J. Ding, N. Pelakanos, A. V. Nurmikko, H. Luo, N. Samarth, and J. K. Furdyna, Appl. Phys. Lett. **57**, 2885 (1990).
[25] N. T. Pelakanos, H. Haas, N. Magnea, H. Mariette, and A. Wasiela, Appl. Phys. Lett. **61**, 3154 (1992).
[26] M. Heuken, J. Söllner, F. E. G. Guimarães, K. Marquardt, and K. Heime, J. Cryst. Growth **117**, 336 (1992).
[27] C. Gerardi (private communication).
[28] R. S. Knox, *Theory of Excitons*, Solid State Physics, Suppl. 5 (Academic, New York, 1963).
[29] C. Benoit à la Guillaume, J. M. Debever, and F. Salvan, Phys. Rev. B **38**, 567 (1969).
[30] J. Valenta, D. Guennani, A. Manar, B. Hönerlage, T. Cloitre, and R. L. Aulombard, Solid State Commun. **98**, 695 (1996).
[31] D. Guennani, J. Valenta, A. Manar, J. B. Grun, T. Cloitre, O. Briot, and R. L. Aulombard, Solid State Commun. **96**, 637 (1995).
[32] J. Gutowski, I. Broser, and G. Kudlek, Phys. Rev. B **39**, 3670 (1989).
[33] R. Baltrameyunas and É. Kuokshtis, Fiz. Tverd. Tela (Leningrad) **22**, 1009 (1980) [Sov. Phys. Solid State **22**, 589 (1980)].
[34] G. Beni and T. M. Rice, Phys. Rev. B **18**, 768 (1978).